LETTER TO THE EDITOR

Stretching of proteins in a force-clamp

P Szymczak[1] **and Marek Cieplak**[2]

[1] Institute of Theoretical Physics, Warsaw University, ulica Hoża 69, 00-681 Warsaw, Poland
[2] Institute of Physics, Polish Academy of Sciences, Aleja Lotników 32/46, 02-668 Warsaw, Poland

Abstract
Mechanically induced protein unfolding in the force-clamp apparatus is shown, in a coarse-grained model of ubiquitin, to have lognormal statistics above a threshold force and exponential statistics below it. Correspondingly, the mean unfolding time is slowly varying and exponentially decreases as a function of the force. The time dependences of the end-to-end distances are also distinct. The time sequence of unfolding events weakly depends on force and much of it resembles that for stretching at constant speed. A more complicated time dependence arises for integrin.

(Some figures in this article are in colour only in the electronic version)

Atomic force microscopy (AFM) provides a convenient tool with which to mechanically probe biomolecules. Usually, it is employed for stretching at a constant speed. The properties of the force of resistance to stretching, as measured as a function of the AFM tip displacement, yield information about the elastic structure of the biomolecule. Examples of such studies involve titin [1–3] and DNA [4]. Recently, a new variant of AFM has been developed: a force-clamp. This allows one to maintain a constant pulling force on the protein while monitoring the end-to-end distance, L, as a function of time, t. This technique has been used to study unfolding of the domains of titin [5] and polyubiquitin [6, 7]. In the latter case, the end-to-end length of the protein subject to a constant force was found to increase in a step-wise manner with each step corresponding to unwinding of a single ubiquitin chain in agreement with a simple, i.e., two-state all-or-none, model of unfolding. The ensemble-averaged length of a protein is well described by a single exponential with a characteristic time t_{unf} [7]. The logarithm of t_{unf} was shown to depend linearly on the force F. In the present study we investigate the generality of these results. In particular, we show that the average unfolding time needs not to be exponential (especially at large forces) and we provide an example of a protein with more than two steps of unfolding at low forces.

One of the results that comes from the constant speed experiments is an estimate of the maximum force, F_{max}, that is needed to unravel the protein. This information can be obtained even from a single pulling trajectory. In a force-clamp experiment, however, a single trajectory, as represented by the $L(t)$ trace, is not very revealing because the sudden jumps in L take place at seemingly random moments. Furthermore, the appearance of the trace does not tell whether
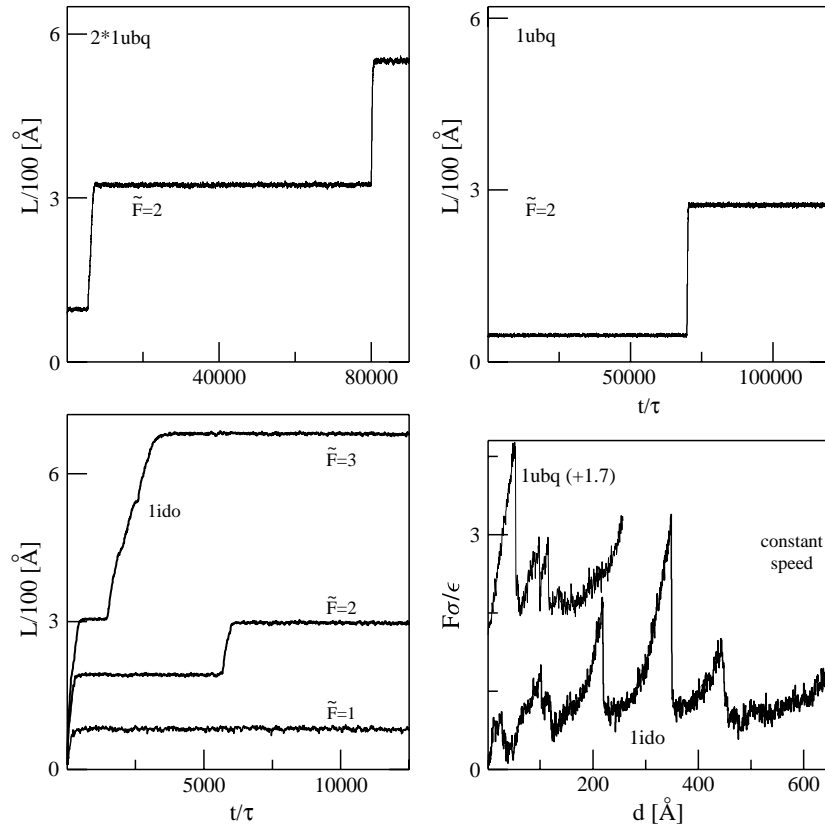
Figure 1. The top two panels show examples of the L versus time trajectories in a constant force protocol. The left- and right-hand panels are for ubiquitin dimer and ubiquitin, respectively. In both cases, $\tilde{F} = 2$, i.e., the force is below F_{max}. The bottom left panel shows three examples of trajectories for integrin at various forces. The lower two trajectories leads to full unfolding at a significantly longer time than the scale in the figure. The Protein Data Bank [14] structure codes for ubiquitin and integrin used here are 1ubq and 1ido, respectively. Ubiquitin consists of 76 amino acids and integrin consists of 192. The bottom right panel shows the force versus displacement traces for stretching performed at constant speed. The trace for ubiquitin is shifted upward by 1.7 to avoid overlap with the trace for integrin. For this trace, $\tilde{F}_{max}$ is near 2.45.

it has been measured above or below F_{max}, especially if F is close to F_{max}. Physical information can be gleaned only by considering ensembles made of many trajectories and determining the properties of distributions of the unfolding times.

Here, we provide a theoretical assessment of the constant-force unfolding experiments from the perspective of a statistical analysis of many trajectories. We focus on ubiquitin and derive distributions of the unfolding times as a function of the force and show that their nature switches from exponential to lognormal on crossing the threshold value F_{max}. Furthermore, we demonstrate that for $F > F_{max}$ the mean unfolding time, t_{unf}, is almost independent of the force, but it grows exponentially on lowering the force for $F < F_{max}$. The fact that on crossing F_{max} the kinetics of unfolding is changed is not surprising in itself. However, the purpose of this paper is to quantify the character of the statistical change. In particular, we demonstrate the existence of different time dependences of the ensemble-averaged L for above and below F_{max}.
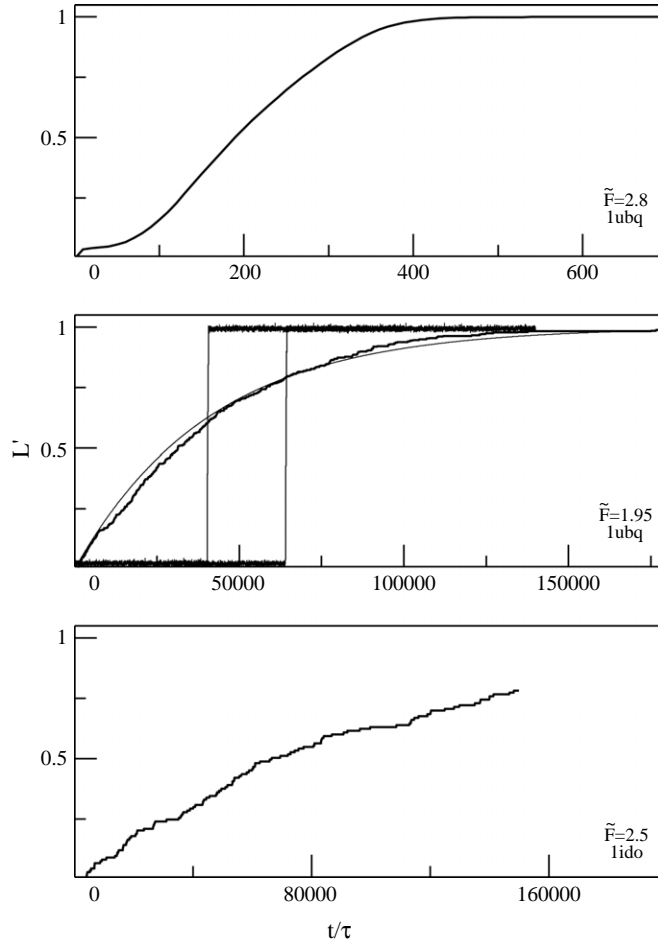
Figure 2. The average normalized end-to-end length, $L' = \frac{L-L_{\mathrm{f}}}{L_{\mathrm{u}}-L_{\mathrm{f}}}$, as a function of time. The top two panels are for single molecules of ubiquitin where the average is over 380 trajectories. In this case, $L_{\mathrm{u}} = 37.1$ Å and $L_{\mathrm{f}} = 288$ Å. The top panel corresponds to $F > F_{\mathrm{max}}$ and the middle panel to $F < F_{\mathrm{max}}$. In the middle panel, two examples of individual step-wise trajectories are also shown. The exponential fit corresponds to $t_{\mathrm{unf}} = 0.32 \times 10^5 \tau$. The data for integrin are shown in the bottom panel. For integrin, $L_{\mathrm{f}} = 10.82$ Å and $L_{\mathrm{u}} = 699$ Å.

Proteins, when stretched at a constant speed, usually exhibit several force maxima, and one of them is often clearly dominant. In the case of ubiquitin and the I27 domain of titin the dominant peak is the first significant maximum that comes as a function of the displacement, d [8, 9]. However, one can find proteins, like integrin, for which the dominant peak force corresponds to a later maximum. We show that this feature complicates the behaviour of the unfolding characteristics still further.

It is difficult to generate a theoretical account of unfolding in the force-clamp apparatus using all-atom simulations. Not only are the timescales required for single trajectory unfolding simulations orders of magnitude too long, but also there is an intrinsic necessity to consider many unfolding processes in order to discuss ensembles. Go-like models [10, 11] offer a means of rescue in this context. We focus on ubiquitin and integrin as case studies and model the two proteins in the Go-like fashion. We follow the implementation as outlined
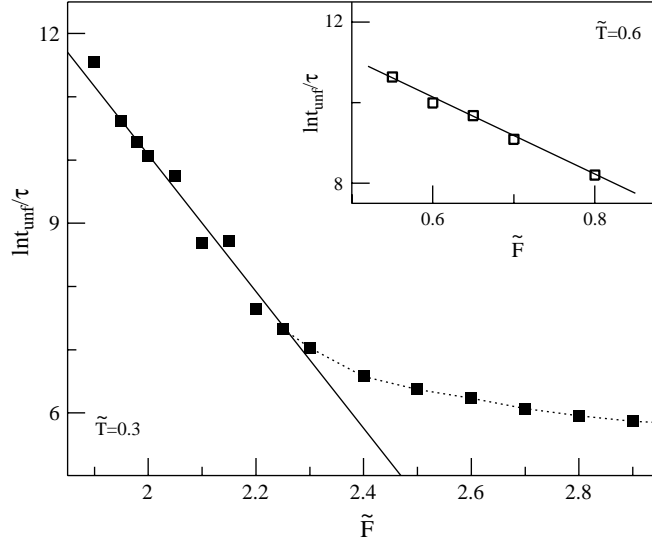
Figure 3. The mean unfolding time, t_{unf}, for ubiquitin, as a function of the dimensionless force. $\tilde{F}_{max}$ is close to 2.4 at $\tilde{T} = 0.3$. The solid line indicates the slope valid for $F < F_{max}$ and the dotted line for $F > F_{max}$. The two lines intersect near F_{max}. The inset shows the exponential regime seen at a higher temperature of $\tilde{T} = 0.6$.

in [12, 8] and, specifically for ubiquitin, in [9]. The latter paper discusses stretching and constant speed. The model consists of a chain of self-interacting C^α atoms that are tethered by harmonic potentials with minima at 3.8 Å. The other interactions are selected so that the global energy minimum agrees with the experimentally established native conformation. The interactions, called contacts, can be divided into native and non-native kinds by checking atomic overlaps in the native conformation as described by Tsai *et al* [13]. In order to prevent the emergence of entanglements, the non-native contacts are endowed with a hard core repulsion at a distance of $\sigma = 5$ Å. The native contacts are described by the Lennard-Jones potentials $V_{ij} = 4\epsilon[(\frac{\sigma_{ij}}{r_{ij}})^{12} - (\frac{\sigma_{ij}}{r_{ij}})^6]$, where the length parameters σ_{ij} are chosen so that the potential minima correspond to the native distances between the C^α atoms i and j. The energy parameter, ϵ, is taken to be uniform, and its effective value for titin and ubiquitin appears to be of order 900 K, so the reduced temperature, $\tilde{T} = k_B T/\epsilon$, of 0.3 ($k_B$ is the Boltzmann constant and T is temperature) should be close to the room-temperature value [9]. Unless mentioned otherwise, all results are obtained for this value of $\tilde{T}$. In our stretching simulations, the N-terminus of the protein is attached to harmonic springs of elastic constant $k = 0.06\epsilon/\text{Å}^2$. The C-terminus is pulled by a force, F. In the constant speed simulations, the C-terminus is attached to another harmonic spring with the same k as at the N-terminus. The other end of the C-terminus spring moves at a speed $v_p = 0.005$ Å/τ, where $\tau = \sqrt{m\sigma^2/\epsilon}$ is the characteristic time unit and m is the average mass of the amino acids.

Thermostating is provided by the Langevin noise which also mimics random kicks by molecules of the implicit solvent. An equation of motion for each C^α reads $m\ddot{\mathbf{r}} = -\gamma\dot{\mathbf{r}} + F_c + \Gamma$, where F_c is the net force on an atom due to the molecular potentials and Γ is a Gaussian noise term with dispersion $\sqrt{2\gamma k_B T}$. The damping constant γ is taken to be equal to $2m/\tau$ and the dispersion of the random forces is equal to $\sqrt{2\gamma k_B T}$. This choice of γ corresponds to a situation in which the inertial effects are negligible [12]. In order to make the damping as effective as in water, γ should be about 25 times larger and the resulting timescales would
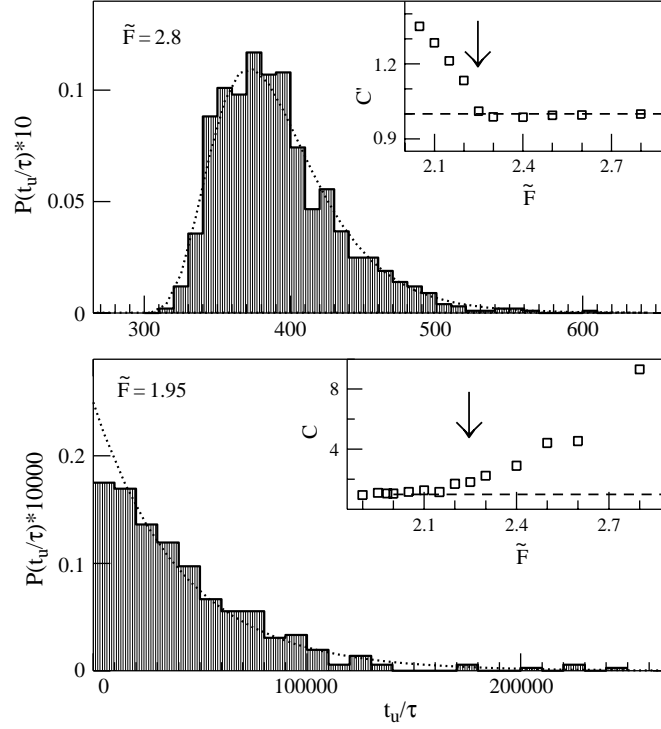
Figure 4. Distributions of unfolding times for ubiquitin. The top panel is for $\tilde{F} = 2.8$ and it corresponds to 1000 processes. The dotted line indicates a fit to a lognormal distribution $P(t/\tau) = \frac{1}{\sqrt{2\pi}\sigma(t-t_0)}\exp{-\frac{\ln^2(\frac{t-t_0}{m})}{2\sigma^2}}$, with t_0, σ, and m equal to 280τ, 0.37, and 105τ respectively, and t is short for the unfolding time t_u such that $t_{unf} = \langle t_u \rangle$. The inset shows $C' = (\frac{\langle t^2 \rangle}{\langle t \rangle^2})^3 \frac{\langle t \rangle^3}{\langle t^3 \rangle}$ as a function of $\tilde{F}$. The unit value of C', seen for $\tilde{F} > 2.25$, is indicative of the lognormal distribution. The bottom panel is for $\tilde{T} = 1.95$, i.e., for an F below F_{max}. The data are based on 380 processes. The dotted line shows a fit to an exponential distribution $P(t) = \frac{1}{t_{unf}}\exp{-t/t_{unf}}$ with $t_{unf} = 0.32 \times 10^5\tau$. The inset shows $C = \frac{\langle t \rangle}{\sigma_t}$, where σ_t denotes the dispersion in the distribution of t, as a function of $\tilde{F}$. A unit value of C is indicative of the exponential nature of the probability distribution.

become about 25 times longer [12]. The equations of motion are solved by a fifth-order predictor–corrector scheme.

Three panels of figure 1 show examples of the $L(t)$ trajectories for ubiquitin, a ubiquitin dimer, and integrin. The time evolution consists of steps in L until the ultimate extension is reached. For ubiquitin, there is just one step. For two-ubiquitin, there is a serial unwinding of the domains and thus two steps in L. The example traces for ubiquitin and two-ubiquitin are for the dimensionless force, $\tilde{F} = F\sigma/\epsilon$, of 2, which is below $\tilde{F}_{max}$ equal to ~ 2.45. In the case of integrin, one trajectory is for $F > F_{max}$ and two for $F < F_{max}$. The trajectories corresponding to the lower forces are not developed to the full extension within the scale of the figure. It is seen that single integrin allows for multiple steps whereas single ubiquitin does not. This difference is explained in the bottom right panel of figure 1 which shows the constant speed results for the force determined against displacement. The biggest force needed to unravel ubiquitin arises at the beginning of the process. On the other hand, in the case of integrin other modules unravel before the biggest force expense takes place. Unwinding of these weaker modules gives rise to multiple steps under the constant-force conditions.
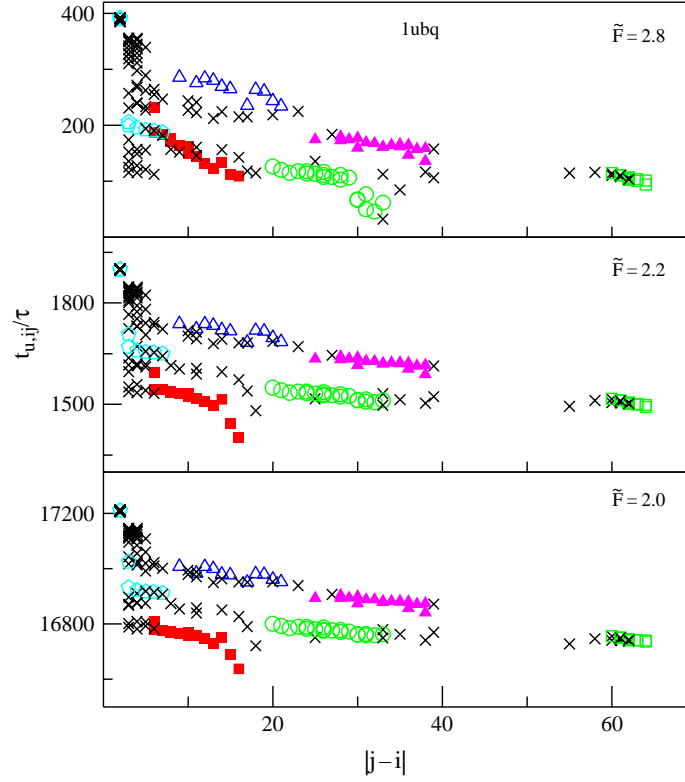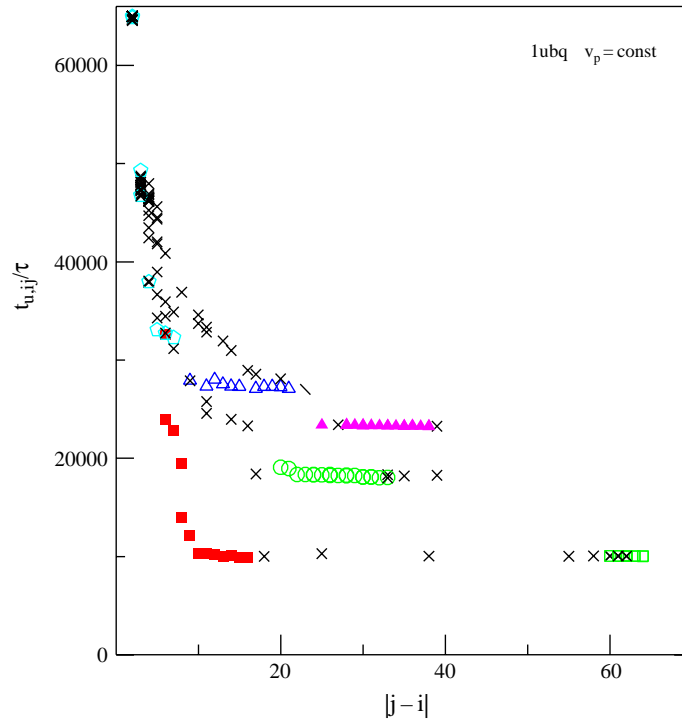
Figure 5. The stretching scenarios at constant force for ubiquitin for forces indicated. The symbols assigned to specific contacts are the same in all panels. Open circles, open triangles, open squares, open pentagons, solid triangles, and solid squares correspond to contacts (36-44)–(65-72), (12-17)–(23-34), [(1-7),(12-17)]–(65, 72), (41-49)–(41-49), (17-27)–(51-59), (1-7)–(12-17) respectively. The crosses denote all other contacts. The segment (23-34) corresponds to a helix. The two β-strands (1-7) and (12-17) form a hairpin. The remaining β-strands are (17-27), (41-49), and (51-59).

Figure 2 shows what happens to L when this quantity is averaged over many trajectories. Instead of L itself, we consider a normalized, and dimensionless, L', defined as $\frac{L-L_f}{L_u-L_f}$, where L_f and L_u stand for the folded and unfolded end-to-end distances, respectively. For $F > F_{max}$, the time dependence of $\langle L' \rangle$ for ubiquitin is sigmoidal, with a point of inflection (the top panel). On the other hand, for $F < F_{max}$, the dependence is exponential with a single timescale given by t_{unf} (the middle panel). This panel also demonstrates that even though individual trajectories are step-wise, an averaging over many trajectories leads to a quantity which is governed by a single exponential, consistent with a two-state behaviour [7].

In the case of integrin (the bottom panel of figure 2), we were not able to run processes to achieve the full unwinding. However, the data averaged over 100 trajectories indicate disappearance of discrete steps also in this case. We expect that the average behaviour could be fitted to a sum of two or three exponentials, depending on the field, but demonstrating this would require significantly larger statistics than available through our simulations.

The qualitative difference between the two force regions becomes more transparent when one considers the average unfolding times (figure 3) and the distributions of the unfolding times (figure 4). Figure 3 shows that the average unfolding time depends on the value of the force

Figure 6. The stretching scenario at constant pulling speed for ubiquitin. The symbols used are as in figure 5.

in the large force region very weakly, possibly becoming force-independent asymptotically. However, it displays an exponential dependence in the small force region. The crossover is around $\tilde{F} = 2.3$, which is close to $F_{\max}$ as derived from one trajectory of the constant speed unwinding. The value of $F_{\max}$ decreases with temperature, which results in shifting the region of the exponential dependence to smaller forces as shown in the inset of figure 3 for $\tilde{T} = 0.6$ for which case $\tilde{F}_{\max} = 0.88$.

Figure 4 demonstrates that the large and small force regions give rise to very different kinds of statistics of the individual unfolding times, t_u. The distribution is lognormal above $F_{\max}$ and exponential below. The crossover between these two statistics can be conveniently illustrated by analysing the moments of the distributions. In the insets of figure 4 we plot certain combinations of the moments of t_u, C and C', defined in the caption, such that C is equal to 1 for the exponentially distributed variable, whereas C'—for the lognormal one. The graphs clearly show a statistical crossover occurring at $\tilde{F} \approx 2.2$–2.3, which is consistent with the result of the average unfolding time analysis (see the arrows in the insets of figure 4).

The occurrence of the crossover can be understood by observing that the unfolding time is actually the sum of two terms: t_1, the waiting time for the unwinding to begin (which is distributed exponentially), and t_2, the duration of the unwinding process itself, which is largely independent of the force (corresponding to the step width in figure 1). For small forces, the unfolding time is dominated by the waiting time, which can be huge. In contrast, for $F > F_{\max}$ the unwinding begins essentially immediately and t_{unf} probes the fine details of the unfolding process. The crossover between the two regimes takes place when t_1 becomes comparable with t_2, which corresponds to the stretching force a bit below $F_{\max}$, just as is seen in the simulations.

Finally, we discuss the unfolding scenarios. These can be characterized [8] by determining average times at which a contact is broken for the last time and plotted versus the contact order, i.e., the sequential separation $|j - i|$ between the C^α atoms that can form a native contact. A contact is said to be broken if a distance of $1.5\sigma_{ij}$ is crossed. Figure 5 shows that the order of rupturing events depends on F rather weakly despite a significant variation in the absolute timescales. This is consistent with the two-stage picture outlined above. It should be noted, however, that there is a slight change in the pattern of points on crossing F_{max} that is easiest to notice in the time sequencing of the hairpin (the solid squares) at $|j - i|$ around 15. It is interesting to point out that the order of unfolding events at constant velocity, see figure 6, is nearly the same as at constant force (at the same temperature of $\tilde{T} = 0.3$). The most visible difference is that the rupture of the helix 41-49 (the open pentagons) comes later than the rupture of the bonds between (12-17) and (23-34) (open triangles).

In conclusion, results of our Go-like model highlight fundamental force-driven crossover in the statistics of unfolding events in experiments that involve the force-clamp AFM.

References

[1] Rief M, Gautel M, Oesterhelt F, Fernandez J M and Gaub H E 1997 *Science* **276** 1109
[2] Marszalek P E, Lu H, Li H B, Carrion-Vazquez M, Oberhauser A F, Schulten K and Fernandez J M 1999 *Nature* **402** 100
[3] Fowler S B, Best R B, Toca Herrera J L, Rutherford T J, Steward A, Paci E, Karplus M and Clarke J 2002 *J. Mol. Biol.* **322** 841
[4] Bockelmann U, Essevaz-Roulet B and Heslot F 1997 *Phys. Rev. Lett.* **79** 4489–92
[5] Oberhauser A F, Hansma P K, Carrion-Vazquez M and Fernandez J M 2001 *Proc. Natl Acad. Sci. USA* **98** 468
[6] Fernandez J M and Li H 2004 *Science* **303** 1674
[7] Schlierf M, Li H and Fernandez J M 2004 *Proc. Natl Acad. Sci. USA* **101** 7299
[8] Cieplak M, Hoang T X and Robbins M O 2004 *Proteins: Struct. Funct. Bio.* **56** 285
[9] Cieplak M and Marszalek P E 2005 *J. Chem. Phys.* at press
[10] Abe H and Go N 1981 *Biopolymers* **20** 1013
[11] Takada S 1999 *Proc. Natl Acad. Sci. USA* **96** 11698
[12] Cieplak M and Hoang T X 2003 *Biophys. J.* **84** 475
[13] Tsai J, Taylor R, Chothia C and Gerstein M 1999 *J. Mol. Biol.* **290** 253
[14] Berman H M, Westbrook J, Feng Z, Gilliland G, Bhat T N, Weissig H, Shindyalov I N and Bourne P E 2000 *Nucleic Acids Res.* **28** 235–42